IEEE Access
Multidisciplinary | Rapid Review | Open Access Journal

Received July 8, 2020, accepted July 26, 2020, date of publication August 7, 2020, date of current version August 20, 2020.

Digital Object Identifier 10.1109/ACCESS.2020.3015107

A Novel Printed Monopole Antenna With Folded Stepped Impedance Resonator Loading

HONGLIN ZHANG[1,2], (Member, IEEE), DONG CHEN[1], (Member, IEEE), AND CHUNLAN ZHAO[3]

[1]College of Electronic and Optical Engineering, Nanjing University of Posts and Telecommunications, Nanjing 210023, China
[2]College of Microelectronics, Nanjing University of Posts and Telecommunications, Nanjing 210023, China
[3]13th Research Institute, China Electronics Technology Group Corporation, Shijiazhuang 050051, China

Corresponding author: Honglin Zhang (zhlandhsl@163.com)

This work was supported in part by the National Natural Science Foundation of China under Grant U1636108, and in part by the Nanjing University of Posts and Telecommunications Science Foundation (NUPTSF) under Grant NY2019078.

ABSTRACT In this article, a novel printed monopole antenna with folded stepped impedance resonator (SIR) loading is proposed, designed and fabricated with a standard printed circuit board process. The antenna comprises of a printed monopole antenna and a folded SIR with internal coupling etched on the back of the antenna. By loading this folded SIR as a near-field resonant parasitic (NFRP) element, the resonant frequency of the antenna can be reduced by the strong coupling between the folded SIR and the radiation patch of the printed monopole. After reviewing the theoretical analysis of the proposed printed monopole antenna, a prototype antenna has been fabricated and measured. The simulated results agree well with the measured results, and the prediction performance of the antenna is verified. Therefore, the proposed method in this article is a promising candidate for printed monopole antenna design.

INDEX TERMS Printed monopole antenna, near-field resonant parasitic (NFRP), folded stepped impedance resonator (SIR), coupling.

I. INTRODUCTION

With the rapid development of wireless communication systems, antennas as a key component are facing more challenges in terms of lightweight, small size, low cost and ease manufacturing coverage [1], [2]. With the development of integrated circuit and component technology, the size of these devices is decreasing, and the demand for antenna integration is increasing. In recent years, design methods of printed monopole antennas with various structures have been proposed [3]–[10]. For instance: tapered meander line [3], folded meandering branches [4], half-cutting method [5], shorted pin connecting ground [6], meandered split-ring slot [7], loading rectangular patch [8], and coplanar waveguide (CPW) feeding monopole antenna [9], [10].

In [11], a multi-folded taper line monopole antenna proposed. The printed monopole antenna can obtain the impedance matching by folding the space between the strips. Nevertheless, the structure of the antenna is 3-D rather than 2-D, which increases the manufacturing difficulty and cost. In [12], by half-cutting method, a printed monopole antenna is achieved, but its size is still large. In [13], [14], the meandering techniques are utilized to miniaturize the printed monopole antenna, thereby, making the antenna physically and electrically more flexibility to reduce its size. However, the antenna has narrower bandwidth than the compact monopole antenna by other techniques.

For another, near-field resonant parasitic (NFRP) element have been widely used to design printed monopole antennas [15]. In [16], by loading a pair of Egyptian axe dipole as NFRP element, the printed monopole antenna is designed to be completed. In [17], a printed monopole antenna with a capacitively-loaded loop (CLL) as NFRP element is presented. In [18], by placing a meander line that acts as an NFRP element near the printed monopole antenna, the monopole is realized. In [19], a printed monopole antenna is achieved by a single fan-shaped top-loaded monopole as an NFRP element. In [20], a printed monopole antenna with stepped impedance hairpin resonator loading as an NFRP element has been presented.

This article presents a novel design of the printed monopole antenna. By utilizing the strong coupling between the folded

The associate editor coordinating the review of this manuscript and approving it for publication was Tutku Karacolak.

SIR and the radiation patch of the printed monopole antenna, reduction of the resonant frequency of the antenna can be achieved. The folded SIR with internal coupling as a NFRP element is loaded on the back of the monopole antenna, so the size of the antenna is not enlarged. We have carefully reviewed and discussed theoretical analysis and simulated results of the proposed antenna in detail. Finally, the proposed printed monopole antenna is fabricated and measured. The measurement is in good agreement with the predicted results, which verify our design method.

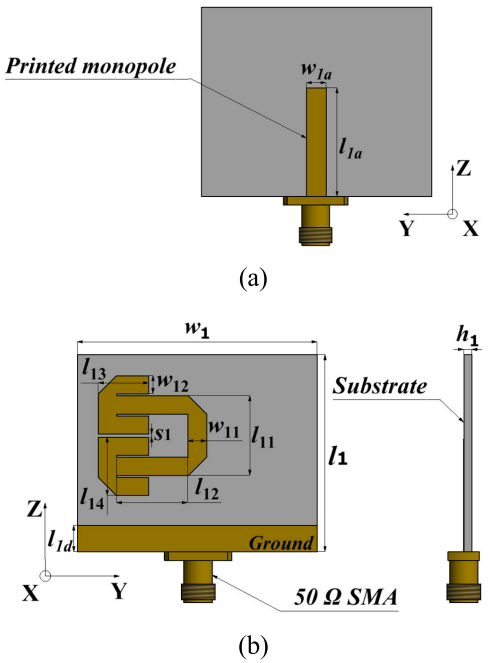

FIGURE 1. Physical layout of the proposed printed monopole antenna. (a) Top view (b) Bottom view.

II. ANTENNA DESIGN

A. ANTENNA CONFIGURATION

In Fig. 1, the preliminary structure of the proposed monopole antenna is illustrated. The radiation patch of the proposed monopole antenna is printed on the top of the substrate, and the folded SIR is constructed at the bottom of the substrate. The antenna is connected to the 50Ω SMA connector. In our design, the antenna is fabricated on a FR4 substrate with a thickness of 0.065 mm and relative dielectric constant and loss tangent are 4.3 and 0.0027, respectively. The sizes of the proposed antenna are listed in Table 1.

B. DESIGN OF FOLDED SIR

The basic principle of the NFPR antenna is to use parasitic elements in the near field of the antenna to reduce the resonant frequency by the coupling between the parasitic elements and the antenna [15]. In our design, the proposed folded SIR is used as NFPR. In Fig. 2, the folded SIR and its equivalent circuit are presented. Two basic SIRs are connected in parallel

TABLE 1. Geometric parametes of the prosed printed monopole antenna.

Parameter	Value	Parameter	Value
w_1	54.0 mm	l_{13}	9.5 mm
w_{1a}	3.8 mm	l_{14}	11.0 mm
l_1	37.0 mm	w_{11}	3.6 mm
l_{1a}	21.2 mm	w_{12}	3.4 mm
l_{1d}	5.0 mm	s_1	0.5 mm
l_{11}	14.9 mm	h_1	0.508 mm
l_{12}	13.5 mm		

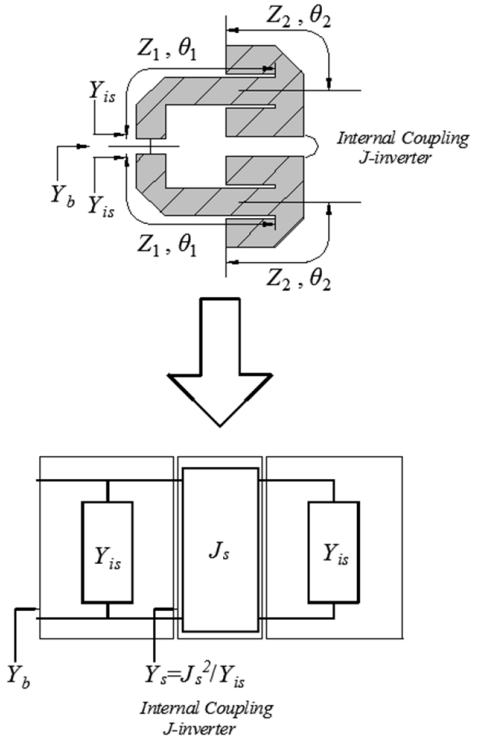

FIGURE 2. The folded SIR and its equivalent circuit.

by internal coupling, so the equivalent circuit includes two admittance Y_{is} and a J-inverter.

Where, Y_{is} can be obtained according to empirical formulas [21],

$$Y_{is} = j\frac{2Z_2 \tan\theta_1 + Z_1 \tan\theta_2}{Z_1(2Z_2 - Z_1 \tan\theta_1 \times \tan\theta_2)} \tag{1}$$

From the basic theory of filter design [22], J-inverter can establish admittance relationship,

$$Y_s = J_s^2/Y_{is} \tag{2}$$

where, the values of J_s can be calculated using the generalized expressions for parallel coupled-lines with arbitrary coupling length in [21].

Y_b is the input admittance of Y_s in parallel with Y_{is} and can be written as follows

$$Y_b = Y_{is} + Y_s = j\begin{cases} \dfrac{2Z_2\tan\theta_1 + Z_1\tan\theta_2}{Z_1(2Z_2 - Z_1\tan\theta_1 \times \tan\theta_2)} \\ -J_s^2 Z_1 \dfrac{2Z_2 - Z_1\tan\theta_1 \times \tan\theta_2}{2Z_2\tan\theta_1 + Z_1\tan\theta_2}) \end{cases} \quad (3)$$

where, Z_1, Z_2, θ_1, and θ_2 are the characteristic impedances and electrical lengths, respectively. From formula (3), we can understand that the input impedance Y_b can be obtained by specifying the required J_s. In our design, J_s is realized by internal coupling of the folded SIR, in other words, the gap S_1.

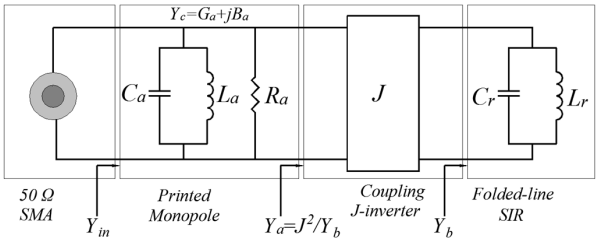

FIGURE 3. The equivalent circuit of the proposed printed monopole antenna.

C. DESIGN OF THE PRINTED MONOPOLE ANTENNA

Fig. 3 depicts the equivalent circuit of the proposed printed monopole antenna with the folded SIR loading. As shown in Fig. 3, the radiation patch of the printed monopole is represented by a lossy shunt resonator composed of R_a, L_a and C_a. Where, R_a equivalent to the radiation resistance of the printed monopole antenna. The gap between the radiation patch of printed monopole antenna and folded-line SIR is considered equivalently as J-inverter.

As mentioned above, the admittance Y_a can be obtained by Y_b and J-inverter,

$$Y_a = J^2/Y_b \quad (4)$$

where, similarly, the values of J can be calculated using the expression in [21].

Then, the admittance of the 'traditional' printed monopole antenna (i.e., without the folded SIR) is extracted by the electromagnetic simulation software CST. As shown in Fig. 2, Y_c can be obtained.

$$Y_c = G_a + jB_a \quad (5)$$

where, G_a and B_a is the real part and imaginary part of admittance Y_c, respectively. Therefore, Y_a, Y_c and Y_{in} have established a parallel relationship,

$$Y_{in} = Y_a + Y_c \quad (6)$$

For convenience, the impedances Z_a, Z_b, Z_c and Z_{in}, which are the reciprocal of the admittance, will be analyzed. The specific sizes of the antenna have been tabulated in Table 1.

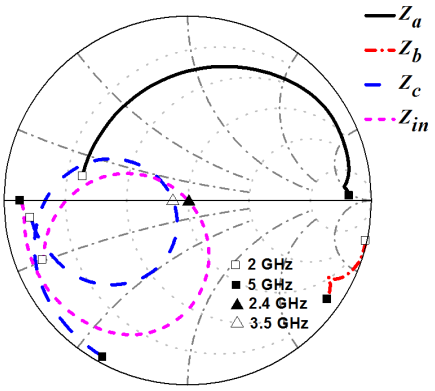

FIGURE 4. Impedance matching procedure of the proposed printed monopole antenna.

As showed in Fig. 4, the calculated results of impedance Z_a, Z_b, Z_c and Z_{in} are presented. As shown in Fig. 4, the imaginary part of the impedance Z_b is capacitive (the imaginary part is negative), since passes through the J-inverter, the imaginary part of the obtained impedance Z_a is inductive (the imaginary part is positive), indicating that their impedance forms a J-inverter. Z_{in} is obtained by capacitance coupling (i.e., inverter J) between the SIR and printed monopole. Therefore, it also can be seen from Fig. 4 that the resonant frequency decreases from 3.50 GHz to 2.40 GHz, and printed monopole antenna is achieved.

Based on the basic knowledge of filter design, the coupling between the resonators shift the resonant frequencies to the low frequency and high frequency, respectively. The stronger the coupling strength, the more obvious the deviation.

As mentioned above, the resonant frequency varies with the gap between the antenna and the folded SIR. In Fig. 1, we define parameter h_1 as the gap between the antenna and the folded SIR.

Several simulations have been carried out to explain this phenomenon. Under simulation, the size parameters of the proposed antenna are set as follows: $l_1 = 37.0$ mm, $l_{1a} = 21.2$ mm, $l_{1d} = 5.0$ mm, $l_{11} = 14.9$ mm, $l_{12} = 13.5$ mm, $l_{13} = 9.5$ mm, $l_{14} = 11.0$ mm, $w_1 = 54.0$ mm, $w_{1a} = 3.8$ mm, w11 = 3.6 mm, w12 = 3.4 mm, and s1 = 0.5 mm.

Fig. 5 shows the return loss varied with different thickness h_1, which can be used to tune the resonant frequency of the monopole antenna. Meanwhile, the simulated S-parameters of a traditional printed monopole antenna without such NFRP is also plotted in Fig. 5. As can be seen from Fig. 5, the resonant frequency of the antenna loaded by the folded SIR continuously moves to the lower frequency band with the decreases of the parameter h_1. That is to say, the stronger the coupling between the folded SIR and printed monopole antenna (the smaller the gap), the lower the resonant frequency of the monopole antenna. Obviously, in Fig. 5, compared to that of the traditional printed monopole antenna, the resonant frequency of monopole antenna with folded SIR is dramatically reduced.

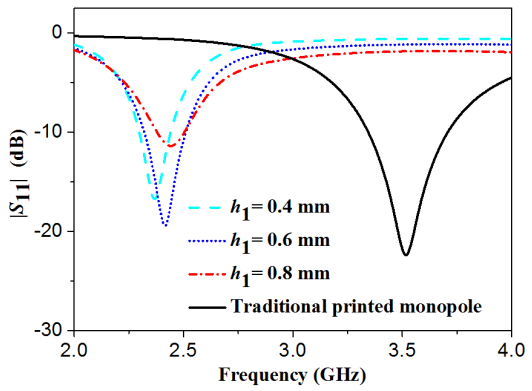

FIGURE 5. The simulated S_{11} varies with h_1.

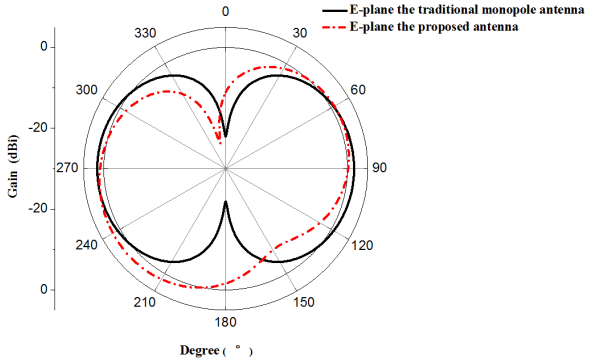

FIGURE 6. The comparison of the simulated E-plane pattern between the proposed antenna and traditional monopole antenna at 2.4 GHz.

D. IMPROVED VERSION OF THE PROPOSED ANTENNA

Based on the analysis above, the radiation pattern of the proposed antenna has been simulated and drawn in Fig. 6. The E-plane pattern of the traditional printed monopole antenna (i.e., remove the folded SIR with internal coupling) at 2.4 GHz has also been simulated and drawn in Fig. 6 for comparison. It can be seen that the maximum radiation direction of the proposed E-plane pattern shifts a certain angle, which is caused by the asymmetry configuration of the antenna.

Under simulation, the size parameters of the proposed antenna are set as follows: $l_1 = 37.0$ mm, $l_{1a} = 21.2$ mm, $l_{1d} = 5.0$ mm, $l_{11} = 14.9$ mm, $l_{12} = 13.5$ mm, $l_{13} = 9.5$ mm, $l_{14} = 11.0$ mm, $w_1 = 54.0$ mm, $w_{1a} = 3.8$ mm, $w_{11} = 3.6$ mm, $w_{12} = 3.4$ mm, $h_1 = 0.508$ mm, and $s_1 = 0.5$ mm.

The radiation pattern can be corrected by symmetrically loading another identical folded SIR on the top of the printed monopole antenna. The physical layout of an improved antenna and its equivalent circuit are shown in Fig. 7 and Fig. 8, respectively. Compared to that in Fig.3, the equivalent circuit has one more parallel resonant circuit as shown in Fig.8.

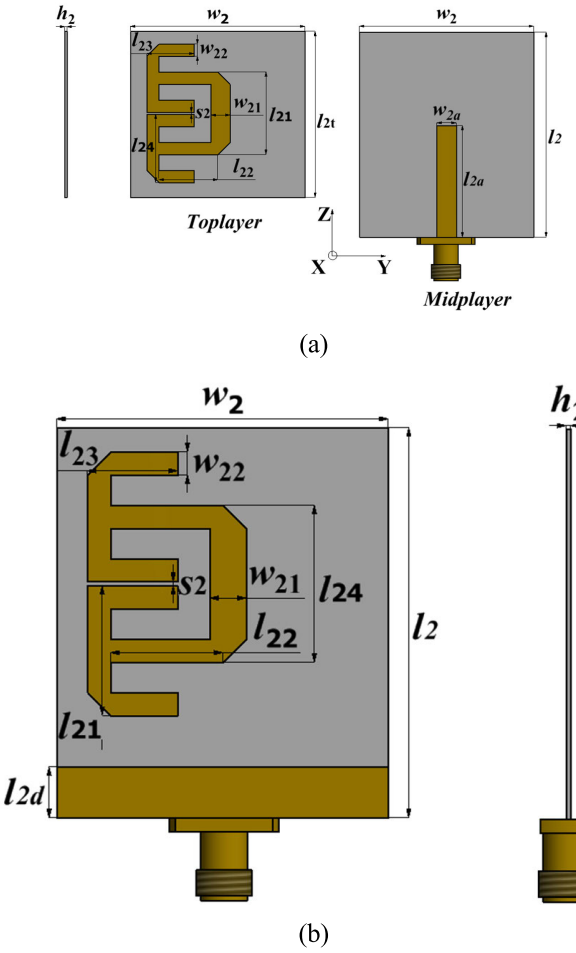

FIGURE 7. Physical layout of the improved printed monopole antenna. (a) Top view (b) Bottom view.

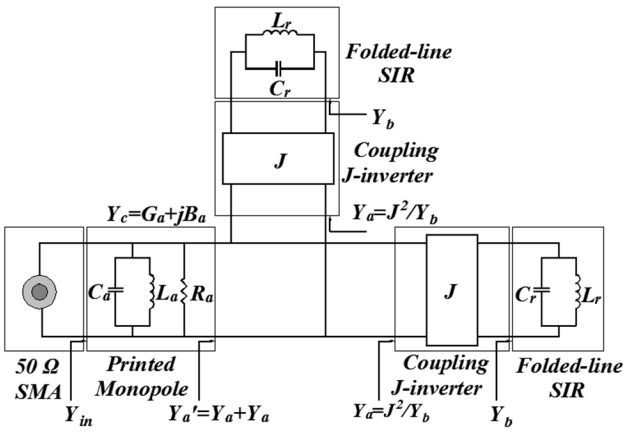

FIGURE 8. The equivalent circuit of the improved printed monopole antenna.

Similarly, the E-plane pattern of the improved antenna is simulated and shown in Fig. 9. The specific sizes of the antenna are listed in Table 2.

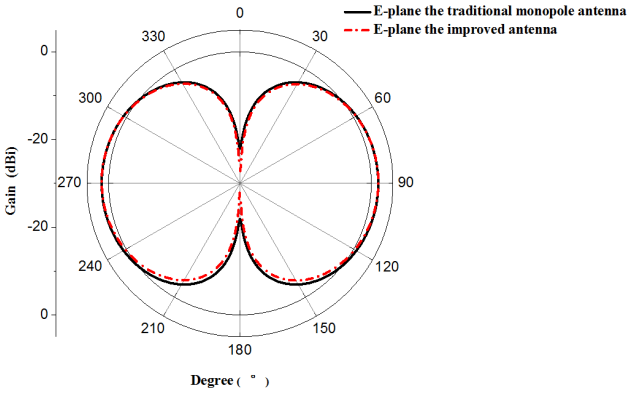

FIGURE 9. The comparison of the simulated E -plane pattern between the improved antenna and traditional monopole antenna at 2.0 GHz.

TABLE 2. Eometric parametes of the prosed printed monopole antenna.

Parameter	Value	Parameter	Value
w_2	38.0 mm	l_{23}	10.3 mm
w_{2a}	4.22 mm	l_{24}	18.1 mm
l_2	45.0 mm	w_{21}	4.2 mm
l_{2a}	24.5 mm	w_{22}	2.7 mm
l_{2d}	5.9 mm	s_2	0.5 mm
l_{21}	14.5 mm	h_2	0.508 mm
l_{22}	12.9 mm	l_{2t}	36.5 mm

As seen from the simulated results in Fig. 9, the E-plane radiation pattern is consistent to that of the traditional printed monopole antenna.

As seen from the simulated results in Fig. 9, the E-plane radiation pattern is consistent to that of the traditional printed monopole antenna.

III. MEASURED RESULTS

In order to verify the designed printed monopole antenna, two sample monopole antennas have been fabricated and measured. After optimization by electromagnetic simulation software CST, the size parameters of the antenna are listed in Table 1 and Table 2, respectively. Meanwhile, the photographs of the fabricated antennas are shown in Fig.10.

The reflection coefficient and radiation pattern were measured by Keysight E5071C vector network analyzer and SATIMO near-field antenna measurement system, respectively.

Both the simulated and measured *S*-parameters are shown in Fig.11. As can be seen from Fig.11, the center frequency of the proposed antenna is about 2.51 GHz, and the corresponding value of S_{11} is about -19dB. At the same time, the center frequency of the improved antenna is about 1.85 GHz, and the corresponding value of S_{11} is about -20dB.

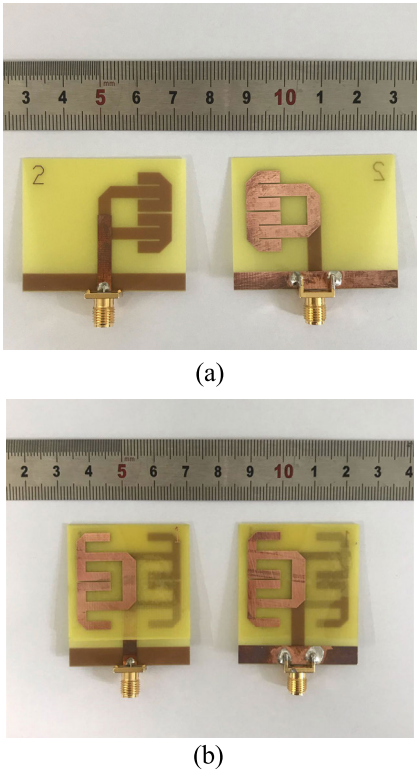

FIGURE 10. Photograph of the printed monopole antenna. (a) The proposed antenna (b) the improved antenna.

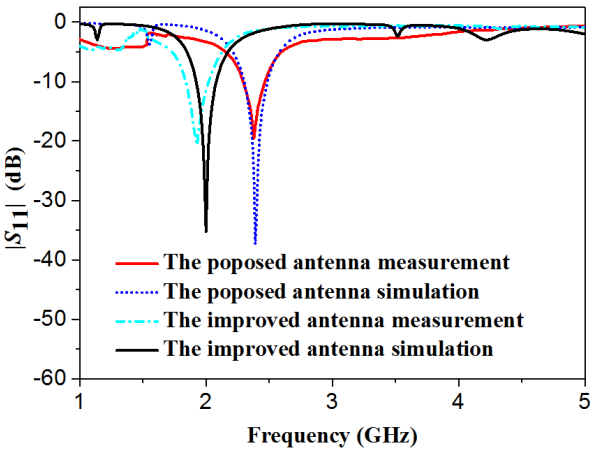

FIGURE 11. Simulated and measured reflection coefficients of the proposed antenna.

The results of simulation and measurement are in good agreement.

As shown in Fig. 12, the simulated and measured gain of the improved monopole antenna are proposed. The measured results show that the antenna has a relatively stable gain over the operating frequency range of 1.6 GHz to 2.2 GHz. The maximum gain is about 1.67dBi, which agree well with the simulated result.

As shown in Fig. 13 and Fig. 14, E-plane and H-plane radiation pattern of the proposed antenna and the

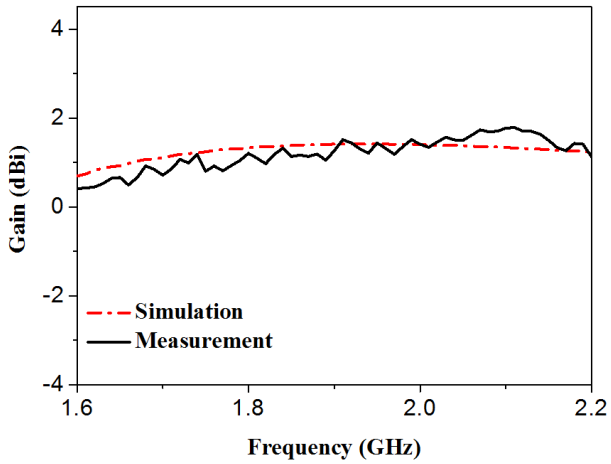

FIGURE 12. Simulated and measured radiation gain of the improved monopole antenna.

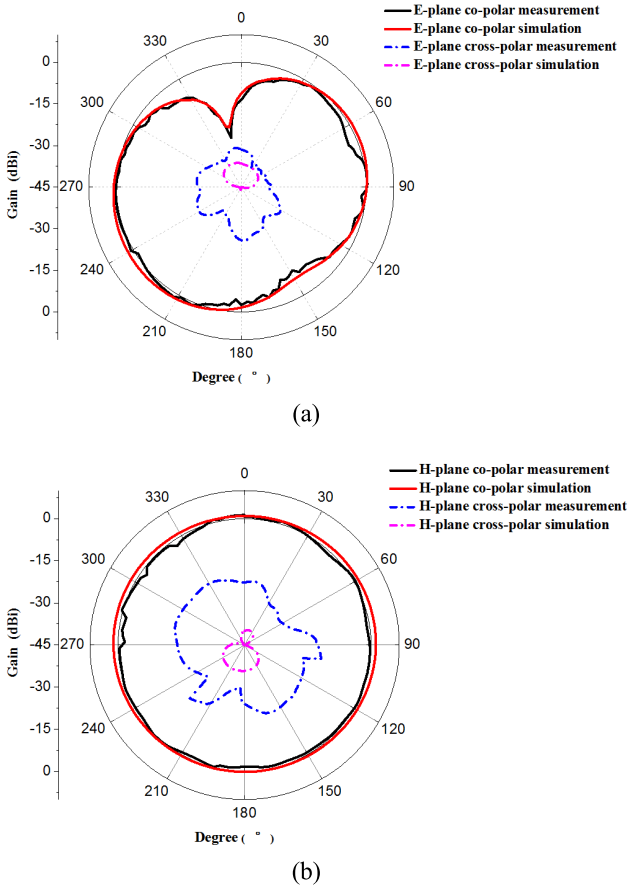

FIGURE 13. Simulated and measured radiation patterns of the proposed antenna at 2.51 GHz (a) E-plane (b) H-plane.

improved antenna at 2.51 GHz and 1.85GHz are given, respectively.

As can be seen from the Fig. 13 and Fig. 14, the antenna has good omnidirectional radiation characteristics over the operating frequency band and low cross polarization performance.

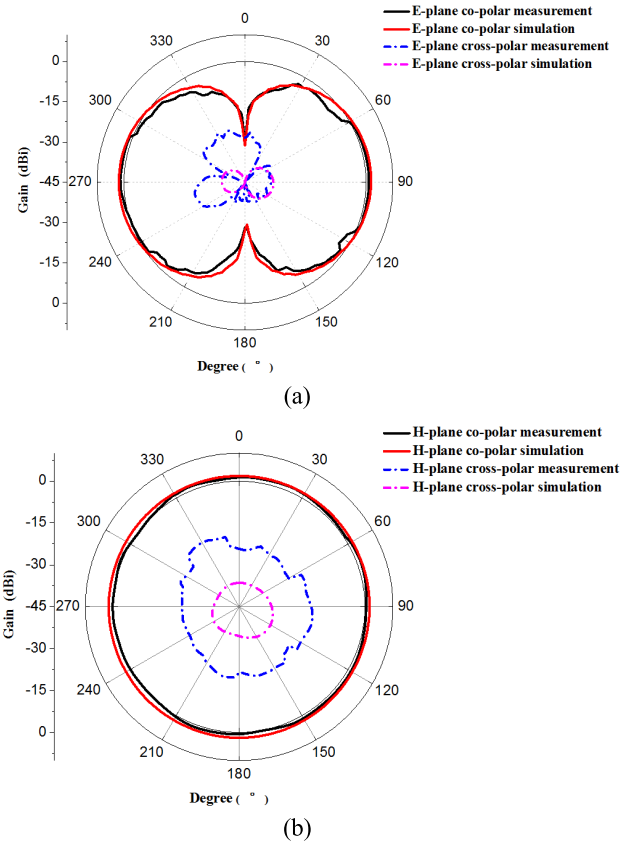

FIGURE 14. Simulated and measured radiation patterns of the improved monopole antenna at 1.85 GHz (a) E-plane (b) H-plane.

IV. CONCLUSION

This article presents a novel printed monopole antenna with folded SIR loading. By utilizing the coupling between the folded SIR and the radiation patch of the printed monopole antenna, the resonant frequency of the antenna can be reduced. The omnidirectional radiation patterns are also presented to verify the satisfactory performance of the proposed antenna. Ultimately, a prototype printed monopole antenna is designed, manufactured and measured. The simulated results are in good agreement with the measured results, which provide a valuable verification for our proposed design method.

REFERENCES

[1] F. Croq and A. Papiernik, "Stacked slot-coupled printed antenna," *IEEE Microw. Guided Wave Lett.*, vol. 1, no. 10, pp. 288–290, Oct. 1991.

[2] J. J. Jun, J. X. Xue, S. H. Feng, and D. Y. Kai, "Compact antenna element for high-resolution SAR polarimetry applications," *Electron. Lett.*, vol. 49, no. 25, pp. 1586–1588, Dec. 2013.

[3] B. Sun, Q. Liu, and H. Xie, "Compact monopole antenna for GSM/DCS operation of mobile handsets," *Electron. Lett.*, vol. 39, no. 22, pp. 1562–1563, Nov. 2003.

[4] P.-L. Teng and K.-L. Wong, "Planar monopole folded into a compact structure for very-low-profile multiband mobile-phone antenna," *Microw. Opt. Technol. Lett.*, vol. 33, no. 1, pp. 22–25, Apr. 2002.

[5] J. Guo, W. Feng, J.-M. Friedt, Q. Zhao, and M. Sato, "A half-cut compact monopole antenna for SFCW radar-based concrete wall monitoring with a passive cooperative target," *IEEE Geosci. Remote Sens. Lett.*, vol. 17, no. 6, pp. 973–977, Jun. 2020.

[6] M. S. Ellis, A.-R. Ahmed, J. J. Kponyo, J. Nourinia, C. Gbobadi, and B. Mohammadi, "Miniaturised printed monopole antenna with a linked ground plane and radiator," *Electron. Lett.*, vol. 54, no. 11, pp. 676–678, Jun. 2018.
[7] P. Liu, Y. Zou, B. Xie, X. Liu, and B. Sun, "Compact CPW-fed tri-band printed antenna with meandering split-ring slot for WLAN/WiMAX applications," *IEEE Antennas Wireless Propag. Lett.*, vol. 11, pp. 1242–1244, Oct. 2012.
[8] C.-Y. Huang and E.-Z. Yu, "A slot-monopole antenna for dual-band WLAN applications," *IEEE Antennas Wireless Propag. Lett.*, vol. 10, pp. 500–502, May 2011.
[9] R. K. Saini, S. Dwari, and M. K. Mandal, "CPW-fed dual-band dual-sense circularly polarized monopole antenna," *IEEE Antennas Wireless Propag. Lett.*, vol. 16, pp. 2497–2500, Jul. 2017.
[10] K. Ding, Y.-X. Guo, and C. Gao, "CPW-fed wideband circularly polarized printed monopole antenna with open loop and asymmetric ground plane," *IEEE Antennas Wireless Propag. Lett.*, vol. 16, pp. 833–836, Sep. 2017.
[11] I. F. Chen and C. M. Chiang, "Multi-folded tapered monopole antenna for wideband mobile handset applications," *Electron. Lett.*, vol. 40, no. 10, pp. 577–578, May 2004.
[12] M. Sun, Y. Ping Zhang, and Y. Lu, "Miniaturization of planar monopole antenna for ultrawideband radios," *IEEE Trans. Antennas Propag.*, vol. 58, no. 7, pp. 2420–2425, Jul. 2010.
[13] H. Zhai, Z. Ma, Y. Han, and C. Liang, "A compact printed antenna for triple-band WLAN/WiMAX applications," *IEEE Antennas Wireless Propag. Lett.*, vol. 12, pp. 65–68, Jan. 2013.
[14] Y. Xu, Y.-C. Jia, and Y.-C. Luan, "Compact CPW fed printed monopole antenna triple band characteristics for WLAN/WiMAX applications," *Electron. Letters.*, vol. 48, no. 24, pp. 1519–1520, Nov. 2012.
[15] R. W. Ziolkowski, "Efficient electrically small antenna facilitated by a near-field resonant parasitic," *IEEE Antennas Wireless Propag. Lett.*, vol. 7, pp. 581–584, May 2008.
[16] M.-C. Tang, B. Zhou, Y. Duan, X. Chen, and R. W. Ziolkowski, "Pattern-reconfigurable, flexible, wideband, directive, electrically small near-field resonant parasitic antenna," *IEEE Trans. Antennas Propag.*, vol. 66, no. 5, pp. 2271–2280, Mar. 2018.
[17] M.-C. Tang, R. W. Ziolkowski, S. Xiao, M. Li, and J. Zhang, "Frequency-agile, efficient, near-field resonant parasitic monopole antenna," *IEEE Trans. Antennas Propag.*, vol. 62, no. 3, pp. 1479–1483, Mar. 2014.
[18] V. Jantarachote, S. Chalermwisutkul, K. Schraml, and D. Heberling, "Comparison of meander line and NFRP miniaturization techniques for RFID on-chip antennas," in *Proc. Int. Symp. Antennas Propag. (ISAP)*, Nov. 2017, pp. 1–2.
[19] M.-C. Tang, Y. Duan, Z. Wu, X. Chen, M. Li, and R. W. Ziolkowski, "Pattern reconfigurable, vertically polarized, low-profile, compact, near-field resonant parasitic antenna," *IEEE Trans. Antennas Propag.*, vol. 67, no. 3, pp. 1467–1475, Mar. 2019.
[20] D. Chen, H. Zhang, and C. Zhao, "A novel printed monopole antenna with stepped impedance hairpin resonator loading," *IEEE Access*, vol. 8, pp. 96975–96980, May 2020.
[21] M. Makimoto and S. Yamashita, *Microwave Resonators and Filters for Wireless Communication: Theory, Design and Application*. Berlin, Germany: Springer, 2001.
[22] D. M. Pozar, *Microwave Engineering*, 4th ed. Hoboken, NJ, USA: Wiley, 2011.

HONGLIN ZHANG (Member, IEEE) received the B.S. degree in telecommunications engineering and the M.S. degree in electrical and information engineering from Hebei University, Baoding, China, in 2005 and 2010, respectively. He is currently pursuing the Ph.D. degree in microelectronics and solid state electronics with the Nanjing University of Posts and Telecommunications, Nanjing, China.

DONG CHEN (Member, IEEE) received the Ph.D. degree in electronic engineering from the Nanjing University of Posts and Telecommunications, Nanjing, China, in 2010. He has been an Assistant Professor of electromagnetic fields with the Nanjing University of Posts and Telecommunications, since 2014. His current research interests include design of the microwave and RF antenna, transceiver, and power amplifier.

CHUNLAN ZHAO received the B.S. degree in telecommunications engineering from Hebei Polytechnic University, Tangshan, China, in 2008. She is currently with the 13th Research Institute, China Electronic Technology Group Corporation, Shijiazhuang, China.